

REPORT

 OPEN ACCESS

## Context matters: The importance of dimerization-induced conformation of the LukGH leukocidin of *Staphylococcus aureus* for the generation of neutralizing antibodies

Adriana Badarau<sup>a,##</sup>, Harald Rouha<sup>a,##</sup>, Stefan Malafa<sup>a,\*</sup>, Michael B. Battles<sup>b,\*\*</sup>, Laura Walker<sup>b</sup>, Nels Nielson<sup>b</sup>, Ivana Dolezilova<sup>a</sup>, Astrid Teubenbacher<sup>a</sup>, Srijib Banerjee<sup>a,#</sup>, Barbara Maierhofer<sup>a</sup>, Susanne Weber<sup>a</sup>, Lukas Stulik<sup>a</sup>, Derek T. Logan<sup>c</sup>, Martin Welin<sup>c</sup>, Irina Mirkina<sup>a</sup>, Clara Pleban<sup>a</sup>, Gerhild Zauner<sup>a</sup>, Karin Gross<sup>a</sup>, Michaela Jägerhofer<sup>a</sup>, Zoltán Magyarics<sup>a</sup>, and Eszter Nagy<sup>a</sup>

<sup>a</sup>Arsanis Biosciences, Campus Vienna Biocenter, Vienna, Austria; <sup>b</sup>Adimab LLC, Lebanon, NH, USA; <sup>c</sup>SARomics Biostructures AB, Medicon Village, Lund, Sweden

### ABSTRACT

LukGH (LukAB) is a potent leukocidin of *Staphylococcus aureus* that lyses human phagocytic cells and is thought to contribute to immune evasion. Unlike the other bi-component leukocidins of *S. aureus*, LukGH forms a heterodimer before binding to its receptor, CD11b expressed on professional phagocytic cells, and displays significant sequence variation. We employed a high diversity human IgG1 library presented on yeast cells to discover monoclonal antibodies (mAbs) neutralizing the cytolytic activity of LukGH. Recombinant LukG and LukH monomers or a LukGH dimer were used as capture antigens in the library selections. We found that mAbs identified with LukG or LukH as bait had no or very low toxin neutralization potency. In contrast, LukGH dimer-selected antibodies proved to be highly potent, and several mAbs were able to neutralize even the most divergent LukGH variants. Based on biolayer interferometry and mesoscale discovery, the high affinity antibody binding site on the LukGH complex was absent on the individual monomers, suggesting that it was generated upon formation of the LukG-LukH dimer. X-ray crystallography analysis of the complex between the LukGH dimer and the antigen-binding fragment of a very potent mAb (PDB code 5K59) indicated that the epitope is located in the predicted cell binding region (rim domain) of LukGH. The corresponding IgG inhibited the binding of LukGH dimer to target cells. Our data suggest that knowledge of the native conformation of target molecules is essential to generate high affinity and functional mAbs.

**Abbreviations:** AHC, anti-human capture; ATP, adenosine triphosphate; BLI, Biolayer interferometry; BSA, bovine serum albumin; CAPS, 3-(cyclohexylamino)-1-propanesulfonic acid; CD, circular dichroism; CDR, complementarity-determining region; CFU, colony forming unit; CHO, Chinese hamster ovary cells; CS, culture supernatant; ELISA, enzyme-linked immunosorbent assay; ESI-MS, electrospray ionization mass spectrometry; Fab, fragment antigen binding; FCS, fetal calf serum; HBSS, Hank's balanced salt solution; HEPES, N-2-Hydroxyethylpiperazine-N'-2-ethanesulfonic acid; Hla, alpha-hemolysin; HlgAB and CB, gamma-hemolysin AB and CB; IC<sub>50</sub>, half maximal inhibitory concentration; K<sub>d</sub>, equilibrium dissociation constant; k<sub>off</sub>, dissociation rate constant; k<sub>on</sub>, association rate constant; LCD, light chain diversification; LukSF, LukED, LukGH: leukocidins SF, ED and GH; mAb, monoclonal antibody; MOI, multiplicity of infection; MSD, Meso Scale Discovery; PBS, phosphate-buffered saline; PEG, polyethylene glycol; PMNs, polymorphonuclear cells; rmsd, root mean square deviation; RPMI medium, Roswell Park Memorial Institute medium; RPMI-CAS, RPMI supplemented with 1% casamino acids; SEC, size exclusion chromatography; SEM, standard error of the mean

### ARTICLE HISTORY

Received 31 May 2016  
Revised 11 July 2016  
Accepted 15 July 2016

### KEYWORDS

Conformational epitope;  
LukGH; *Staphylococcus aureus*; toxin neutralization;  
X-ray crystal structure

## Introduction

*Staphylococcus aureus* is a pervasive human pathogen, responsible for a broad spectrum of diseases, including life-threatening conditions such as pneumonia, bacteremia and sepsis. The ability of *S. aureus* to survive in almost all human tissues is due to the production of an arsenal of virulence factors aimed at

counteracting the immune system.<sup>1,2</sup> These include the highly potent bi-component leukocidins that subvert the immune response by killing human white blood cells that are recruited to the infection site. Five bi-component leukocidins with lytic activity toward human phagocytic cells have been identified in *S. aureus*: gamma-hemolysins AB and CB (HlgAB, HlgCB),


**CONTACT** Eszter Nagy  [eszter.nagy@arsanis.com](mailto:eszter.nagy@arsanis.com)

\*Present address: Department of Virology, Medical University of Vienna, Vienna, Austria;

\*\*Present address: Geisel School of Medicine at Dartmouth, Hanover, New Hampshire, USA;

#Present address: Boehringer Ingelheim, Vienna, Austria

##These authors equally contributed to this work.

 Supplemental data for this article can be accessed on the publisher's website.

Published with license by Taylor & Francis Group, LLC © Adriana Badarau, Harald Rouha, Stefan Malafa, Michael B. Battles, Laura Walker, Nels Nielson, Ivana Dolezilova, Astrid Teubenbacher, Srijib Banerjee, Barbara Maierhofer, Susanne Weber, Lukas Stulik, Derek T. Logan, Martin Welin, Irina Mirkina, Clara Pleban, Gerhild Zauner, Karin Gross, Michaela Jägerhofer, Zoltán Magyarics, and Eszter Nagy

This is an Open Access article distributed under the terms of the Creative Commons Attribution-Non-Commercial License (<http://creativecommons.org/licenses/by-nc/3.0/>), which permits unrestricted non-commercial use, distribution, and reproduction in any medium, provided the original work is properly cited. The moral rights of the named author(s) have been asserted.

leukocidin ED (LukED), PVL (Panton-Valentine Leukocidin)/leukocidin SF (LukSF) and leukocidin GH (LukGH, also called LukAB).<sup>3,4</sup>

LukSF/PVL was the first identified *S. aureus* bi-component leukocidin.<sup>5</sup> It served as a model to understand how the 2 water-soluble monomers, known as S- and F-subunits, of this toxin family form oligomeric pores in their target cell membranes.<sup>4,6,7</sup> It is the S-component that interacts first with the target cells and then recruits the F-component to form the octameric (4 S- and 4 F-components)  $\beta$ -barrel pore complex.<sup>8,9</sup>

LukGH is the most recently discovered member of this toxin family,<sup>10,11</sup> and proved to be distinct from the others in several respects. While LukS, LukE, HlgA and HlgC (S-components), as well as LukF, LukD and HlgB (F-components) display 68 to 80% amino acid sequence homology, LukH and LukG share only 30 and 40% homology with the other S- and F-components, respectively. Unlike the other leukocidins that are highly conserved among *S. aureus* isolates, LukG and LukH sequences display up to 18% variability, suggesting a unique evolution. The most striking difference is the stable dimer formation of LukG and LukH in solution before contacting the target cells.<sup>12,13</sup> We previously elucidated the structure of the LukGH octamer and identified the molecular features required for dimerization in solution.<sup>12</sup>

Intensive research has recently yielded the identities of the cellular receptors of all leukocidins that are important immune molecules expressed on the surface of phagocytic cells.<sup>4</sup> LukS and HlgC, as well as LukE and HlgA display overlapping receptor recognition, and target complement receptors (C5aR and C5L2) and chemokine receptors (CXCR1 and CXCR2), respectively.<sup>14-16</sup> LukGH has a unique target, CD11b, also a complement receptor (CR3, the  $\alpha$ -subunit of the  $\alpha$ M/ $\beta$ 2 integrin/Mac-1 complex) that is expressed by professional phagocytic cells.<sup>17</sup> The *lukGH* gene is part of the core *S. aureus* genome, and is present in all isolates.<sup>4</sup> *lukGH* deletion mutant strains exhibit greatly diminished toxicity toward human polymorphonuclear cells (PMNs) in *in vitro* assays, suggesting that LukGH has a substantial contribution to the overall phagocyte killing by *S. aureus*.<sup>10,11,17,18</sup> The high species specificity of LukGH, and its very low toxic activity toward murine phagocytic cells, have hindered efforts to estimate its contribution to disease pathogenesis in the most commonly used murine infection models.<sup>19</sup>

Here, we describe our efforts toward identifying neutralizing antibodies against LukGH using either the single components or the co-expressed complex as antigens. We found that using the LukGH complex for mAb discovery was critical in identifying highly potent neutralizing antibodies. We also investigated the mechanism of action for the most potent mAbs and determined the high resolution structure of a LukGH - Fab complex. The structure confirms that the epitope is located in the rim domain, which is the predicted cell binding region of LukGH based on homology with the other  $\beta$ -barrel pore forming toxins of *S. aureus* that were mapped for cell binding.<sup>8,16</sup>

## Results

### MAb discovery using LukG and LukH monomers

Recombinant LukG and LukH were expressed in *E. coli* using the CA-MRSA USA300 clonal type sequences (TCH1516

strain) as described previously.<sup>12</sup> The mixture of LukG and LukH was highly potent in lysing human PMNs or HL-60 cells differentiated into granulocytes (Fig. S1).

Biotinylated LukG or LukH monomers were used as baits for the selection of full-length human IgG1 presented on the surface of yeast cells (as described in the Materials and Methods). The antibody library was generated based on naïve human IgG1 gene sequences with  $> 10^{10}$  diversity.<sup>20-24</sup> The best binder yeast clones were used for the expression of soluble IgGs that were purified by Protein A affinity chromatography. MAbs were tested for LukGH neutralizing activity in viability assays with freshly isolated human PMNs or differentiated HL-60 cells. To our surprise, we could not observe significant neutralizing activity with any of the monomer specific mAbs (examples shown with LukG-selected mAbs, Fig. 1A, left panel). When we performed the neutralization assays by pre-incubating the mAbs first with the cognate antigen (LukG or LukH) before adding the other toxin monomer, we detected inhibition of LukGH-mediated cell lysis (examples shown with LukG-selected mAbs, Fig. 1A, right panel). This result was in contrast to those obtained with mAbs selected with other bi-component leukocidin monomers that did not show a difference whether the cognate or both components were pre-incubated with antibodies (example shown for antibodies binding to the F-component of the Panton-Valentine Leukocidin, LukF in Fig. 1B). We also generated polyclonal antibodies against LukG and LukH by immunizing mice with recombinant monomers. Although, the hyper-immune sera had high titers against LukG or LukH based on ELISA and immunoblotting (data not shown), purified IgGs exhibited low neutralizing activity against LukGH. This was improved by  $\sim 20$ -fold when IgGs were first incubated with the monomer used for the immunization, suggesting that the majority of the antibodies were generated against epitopes blocked by LukH in the complex (Fig. S2).

This observation suggested that the binding epitopes recognized by the monoclonal or polyclonal antibodies were most likely masked or hidden upon formation of the LukGH dimer. This was further examined by biolayer interferometry (BLI) analysis. We detected a decrease in both the association rate constant ( $k_{on}$ ) and binding signal (expressed in response units) between antibodies and their cognate antigen upon adding the non-antigen component. The decrease was proportional to the concentration of the non-antigen component, reaching a plateau at a molar ratio of  $\sim 1:1$  of the 2 monomers (example shown in Fig. 2).

We concluded that antibodies that target LukG or LukH as monomers are not suitable for potent neutralization because LukGH exists as a dimer in solution.

### MAbs selected with the LukGH dimer are highly potent in preventing phagocyte lysis

We repeated antibody selection with the yeast libraries using biotinylated LukGH dimer (USA300 CA-MRSA TCH1516 sequence type) co-expressed in *E. coli* as described previously.<sup>12</sup> In contrast to LukG- or LukH-selected mAbs, most antibodies selected with the LukGH dimer (85 in total) displayed neutralizing activity (examples shown in Fig. 3A). Most of the neutralizing naïve mAbs showed detectable

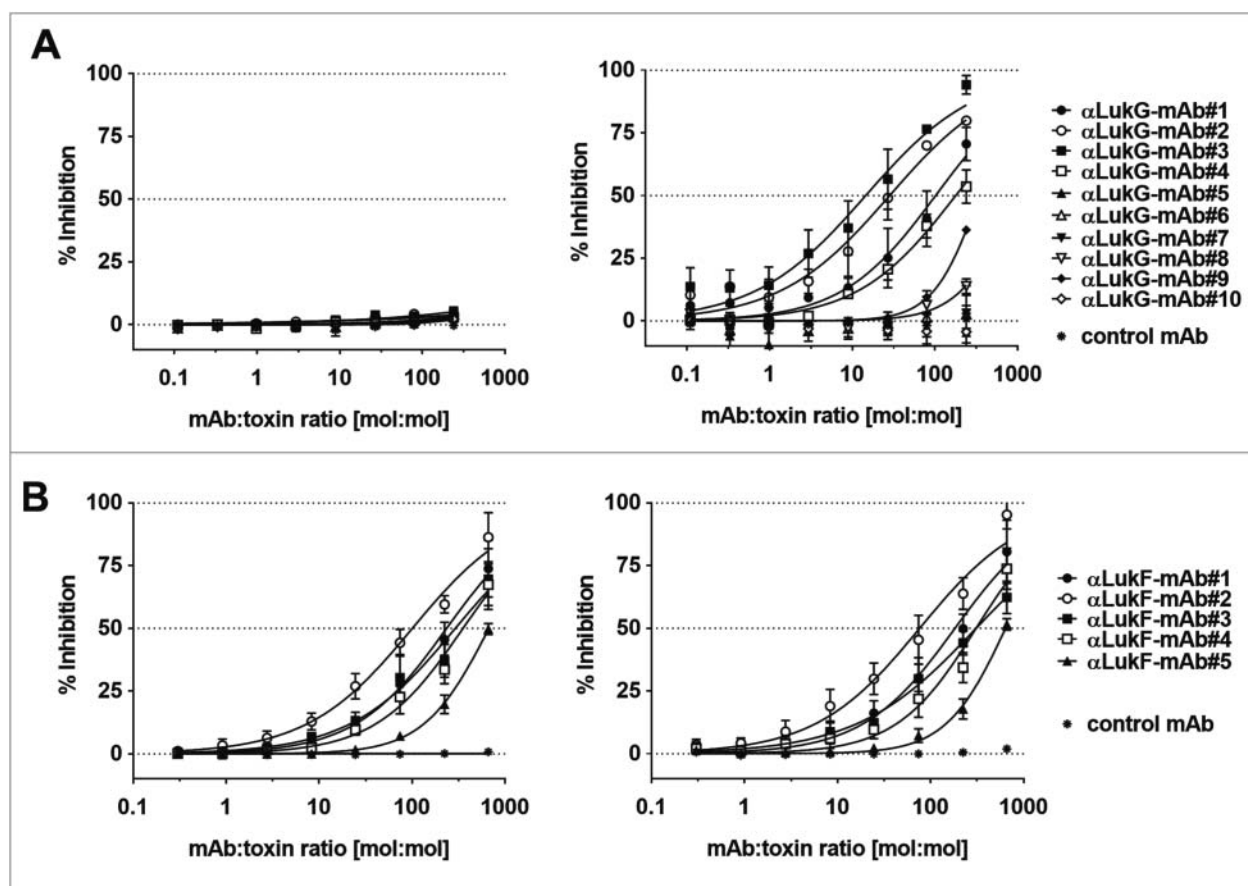


**Figure 1.** Antibodies generated against LukG fail to neutralize LukGH. MAbs selected against the F-components were incubated with both S- and F-components of the respective toxin prior to cell intoxication (left panels). Alternatively, mAbs were pre-incubated with the F-components used for antibody selection before addition of the S-component and the target cells (right panels). (A) naïve yeast derived LukG-selected mAbs (LukGH was used at 7 nM concentration); (B) naïve yeast derived antibodies against LukF (LukSF was used at 2.5 nM concentration). Toxin inhibition was determined in ATP based viability assays using differentiated HL-60 cells. Data represent the means  $\pm$  standard error of the means (SEM) from 2 independent experiments.

binding to either the LukG or the LukH monomer, some to both (in many cases weaker, relative to the LukGH complex), based on BLI measurements. In general, LukG-binder mAbs appeared to be more potent in neutralizing LukGH than the LukH-binders (data not shown).

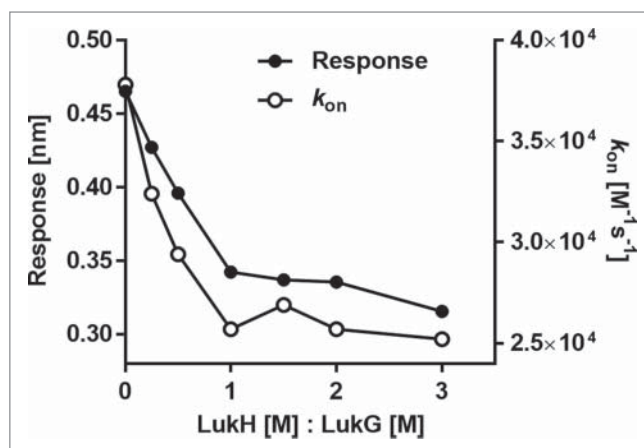


**Figure 2.** LukG and LukH interaction interferes with binding of mAbs generated with monomers. Binding of LukG to  $\alpha$ LukG-mAb#1 immobilized on AHC sensors in presence of different LukH concentrations was measured with BLI. Antigen-antibody complex formation was expressed either as response units or calculated association rate constant ( $k_{on}$ ).

Since LukGH displays significant sequence variation among different *S. aureus* strains (up to 18% differences at the amino acid level), it was important to test cross-reactivity and cross-neutralization with different LukGH variants. We generated LukGH dimers based on gene sequences from 3 additional *S. aureus* strains that are the most distantly related to the USA300 CA-MRSA lineage (CC8/ST8): the MRSA252 (CC30/ST36), MSHR1132 (CC75/ST1850, also called “silver *S. aureus*”), and the livestock-derived H19 (CC10/ST10) strains (sequence comparison shown in Fig. S3). Importantly, all 4 LukGH forms had comparable potency toward human phagocytes, as reported previously by Badarau et al.<sup>12</sup> We detected antibodies that bound and neutralized only the USA300 TCH1516 LukGH variant (e.g.,  $\alpha$ LukGH-mAb#4) used for the yeast selection, but also broadly cross-neutralizing mAbs (e.g.,  $\alpha$ LukGH-mAb#2 and 5) (examples shown in Fig. 3B). Interestingly, the LukG-binder mAbs displayed higher cross-reactivity and cross-neutralization of LukGH variants than LukH-binders (data not shown).

Six of the most potent naïve library-derived antibodies that neutralized all 4 LukGH variants were selected for affinity improvement by subsequent selection with light chain diversified (indicated as LCD) and heavy chain complementarity-determining region (CDR)1 and 2 diversified (indicated as H1H2) libraries in the yeast expression system. Offspring

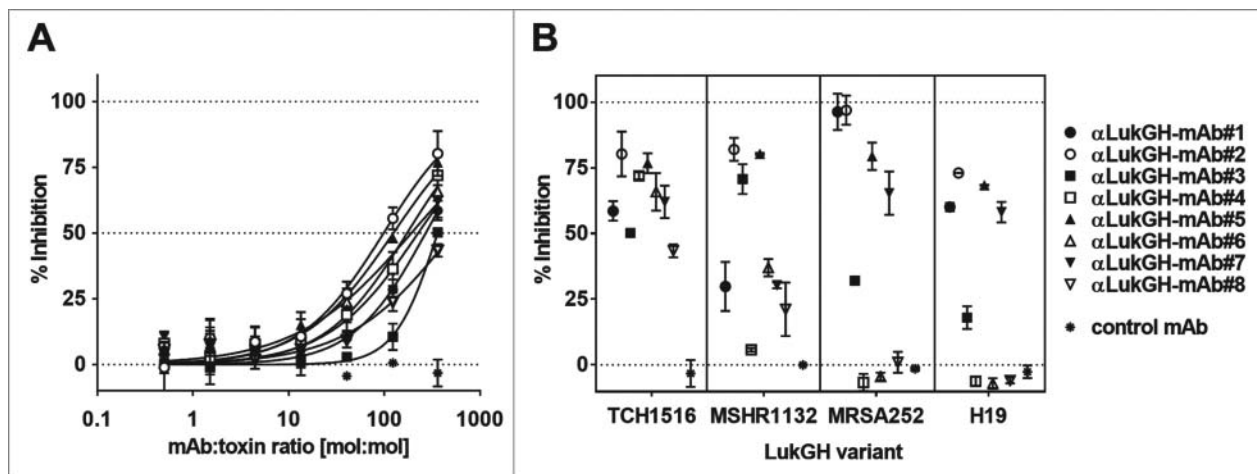


**Figure 3.** MAbs selected with the LukGH dimer prevent neutrophil killing. MAbs selected from naïve yeast surface display libraries with co-expressed biotinylated LukGH were tested for neutralization of LukGH, derived from the TCH1516, MRSA252, MSHR1132 and H19 strains, in PMN viability assays. Co-expressed complexes were used at 1.37 nM; mAbs were tested in the 0.23–500 nM concentration range. (A) Neutralization of TCH1516 LukGH (full titration range). (B) Inhibitory activity of mAbs tested at 500 nM against all 4 LukGH sequence variants. Data are presented as mean values + SEM of 2 independent experiments.

antibodies displayed up to 5000-fold improved affinity and neutralization potency compared to the parental (naïve) antibodies when tested either against recombinant LukGH or the native form of the toxin, secreted into the bacterial culture supernatant (shown with the USA300 LukGH in Fig. 4A). Similar results were obtained with a native LukGH complex purified from the culture supernatant of *S. aureus* strain Newman (Fig. S4). Importantly, these mAbs maintained cross-reactivity and cross-neutralization toward all the different LukGH sequence types tested (H19-type LukGH is shown in Fig. 4B, the MRSA252- and MSHR1132-types are shown in Fig. S5). The neutralizing activity of anti-LukGH antibodies correlated

well with their affinity (Fig. S6). The most potent mAbs with single digit picomolar affinities toward LukGH displayed comparable half-maximal inhibitory concentration ( $IC_{50}$ ) values for all LukGH forms (mAb:toxin ratio at  $IC_{50} < 1$ , example shown in Fig. 5).

The effectiveness of the mAbs was also tested in a neutrophil infection assay. Cells were co-incubated with live bacteria for 2 hours and the effect of *in situ* produced toxins on PMN survival was first measured using a viability dye (Calcein-AM). To assess the contribution of the different cytolytins to PMN toxicity, we tested isogenic *S. aureus* TCH1516 mutant strains lacking *lukGH*, or all other leukocidin genes except *lukGH*, or all 5 leukocidin genes

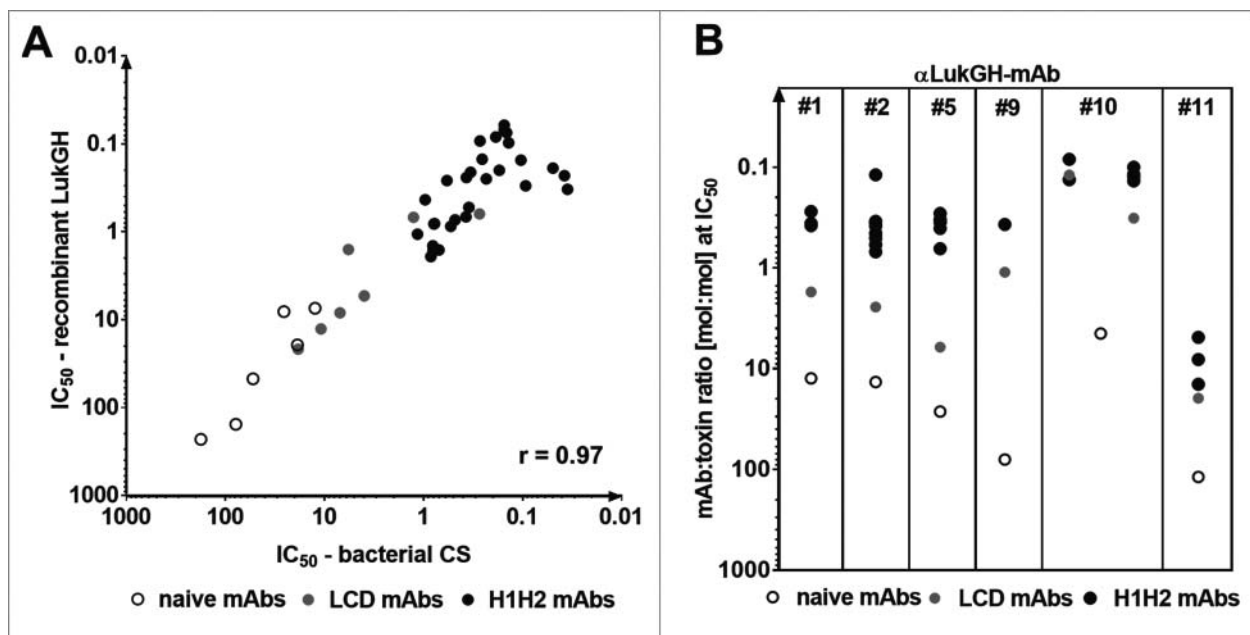


**Figure 4.** Affinity maturation increases neutralizing potency of LukGH mAbs (A) mAbs obtained in 3 selection rounds - naïve, light chain diversification (LCD) and heavy chain CDR1 and/or CDR2 (H1H2) diversification - were tested for neutralization activity against recombinant USA300 LukGH and culture supernatant (CS) from an isogenic TCH1516Δhla-hlgABC-lukED-lukSF strain with human differentiated HL-60 cells. Neutralization potency is expressed as mAb:toxin ratio at  $IC_{50}$  for recombinant LukGH (used at 2.7 nM) and as nM mAb concentration at  $IC_{50}$  for sterile filtered bacterial culture supernatant (used at 16x dilution). Correlation was significant based on Pearson's correlation coefficient analysis ( $r = 0.97$ ,  $p < 0.0001$ ). (B) Neutralization potency of selected mAbs against the H19 LukGH variant used at 0.7 nM with human PMNs is shown as an example.  $IC_{50}$  values were calculated based on 2 independent experiments.

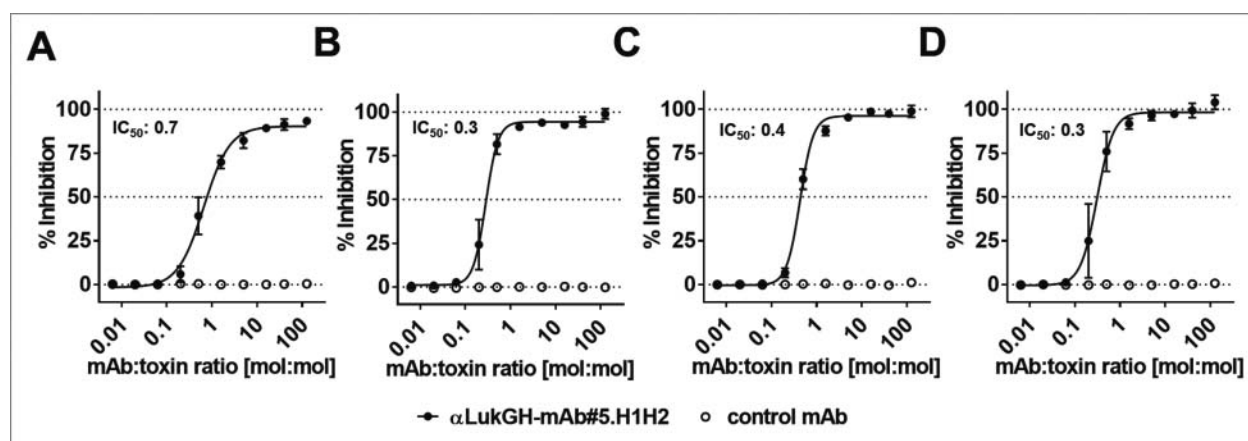


**Figure 5.** Highly potent neutralization of different LukGH sequence variants. Neutralizing activity of  $\alpha$ -LukGH-mAb#5.H1H2 against 4 LukGH variants with differentiated HL-60 cells. Strain (A) USA300 TCH1516, (B) MRSA252, (C) MSHR1132 and (D) H19. Co-expressed complexes were used at 7.5 nM; the mAb was tested in the 0.5–1000 nM concentration range. Data are presented as mean  $\pm$  SEM from 3 independent experiments.

(and  $\alpha$ -hemolysin *hla*). The wild type TCH1516 strain induced dose-dependent toxicity, resulting in < 25% viability of human PMNs at a multiplicity of infection (MOI) of 100 (Fig. 6A). The mutant strain lacking all leukocidin genes had low toxicity ( $\geq 75\%$  cell viability at MOI 100). The *lukGH* deletion strain exhibited toxicity only at high MOIs, while the mutant strain expressing only

the LukGH leucocidin had a comparable effect on PMN survival as the wild type strain, independent of the MOI used (Fig. 6A). Notably the LukGH dependent killing during PMN infection could be neutralized with anti-LukGH mAbs (Fig. 6B). Similar to what we observed in the neutralization assays with recombinant toxins or culture supernatant, the affinity-matured antibodies were more

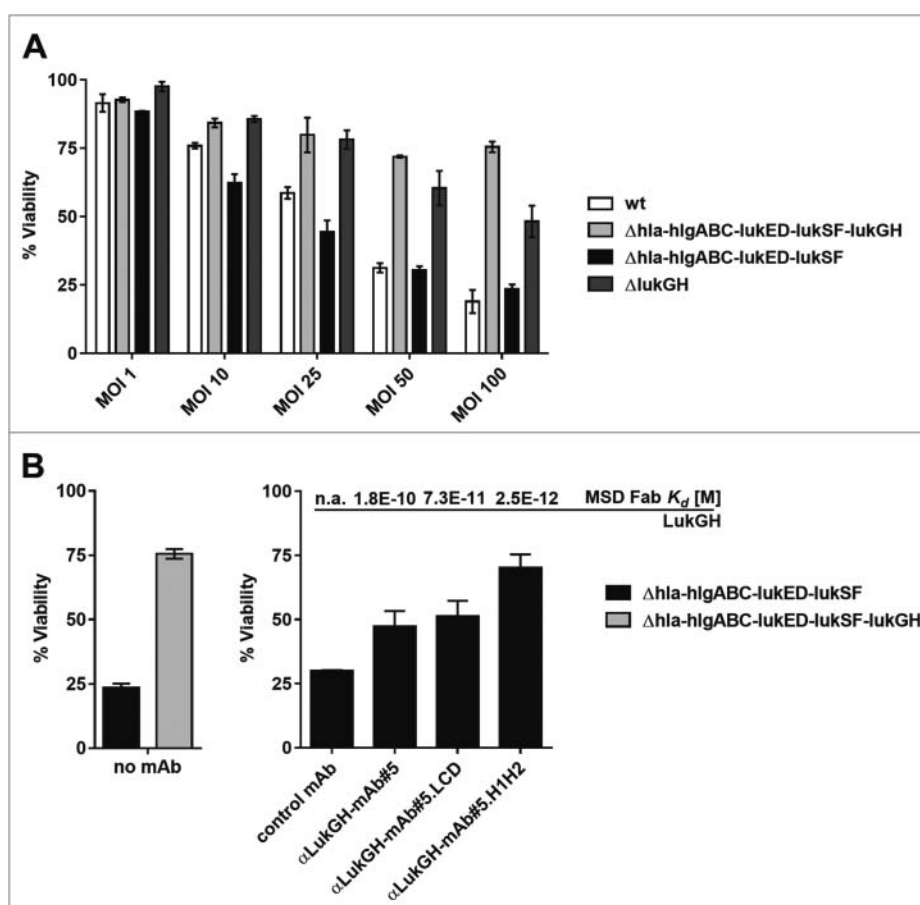


**Figure 6.** Anti-LukGH mAbs inhibit LukGH mediated cell death during *ex vivo* infection of human PMNs. (A) Human PMNs were infected with the indicated wild type and gene deletion mutant *S. aureus* TCH1516 strains at an MOI of 1, 10, 25, 50 and 100 for 2 hours. PMN viability was measured with a Calcein-AM viability dye and is expressed as percentage relative to non-infected control cells. (B) Inhibition of LukGH mediated killing in the presence of indicated mAbs was measured in the same setting using isogenic mutant TCH1516 $\Delta$ *hla-hlgABC-lukED-lukSF* strain at MOI 100 and 195 nM mAb concentration. n.a., not applicable; Data are shown as mean  $\pm$  SEM of 2 independent experiments.

potent compared to the naïve counterparts (examples shown in Fig 6B, right panel).

### LukGH mAbs prevent binding to target cells

To uncover the mode of action of the LukGH neutralizing antibodies, binding of the biotinylated LukGH dimer to PMNs was measured in the absence or presence of the anti-LukGH mAbs using fluorochrome-conjugated streptavidin in a flow-cytometry based surface staining assay. The presence of mAbs correlated with lack of fluorescent surface signal, indicating that LukGH binding to the target cells was inhibited by the mAbs. Importantly, affinity-matured antibodies were more potent than the corresponding naïve (parental) mAbs, and the level of

inhibition was influenced by affinity (examples shown in Fig. 7A). After LukGH associated with its surface target(s), the neutralizing mAbs could not bind any more, suggesting that the epitopes on the heterodimer became hidden upon binding or oligomer formation (Fig. 7B).

### The most potent cross-reactive anti-LukGH mAbs preferentially bind the LukGH complex over the LukG monomer

Since the purpose of this study was to discover mAbs with neutralizing activity across the LukGH variants, we pre-selected those antibodies from the naïve libraries that fulfilled this criterion. To characterize the binding specificity of such mAbs in the LukGH complex, we measured binding response affinity and both the association ( $k_{on}$ ) and the dissociation ( $k_{off}$ ) rate constants, using the LukG and LukH monomers and the co-expressed LukGH complex by BLI. Interestingly, none of these naïve mAbs showed binding to the LukH monomer, but detectable binding to LukG. Six mAbs, selected for affinity maturation, were binned against each other and 4 bins (non-competing mAbs) were identified. We tested representative members of these 4 groups of antibodies and found that all displayed high binding to the co-expressed LukGH, but weak interaction with LukG (2 examples shown in Fig. 8A). For the analysis of affinity-matured antibodies, we employed the Meso Scale Discovery (MSD) method, which measures affinities of components interacting in solution and is typically used for determining very tight binding interactions, in the sub-nanomolar range.<sup>25</sup> The dissociation constants ( $K_d$  values) of the  $\alpha$ LukGH-mAb#5.H1H2 measured by MSD were in the single digit picomolar range with the LukGH complex and the reconstituted LukG+H complex (prepared from the separately expressed LukG and LukH components), confirming their comparable binding to the mAb. The  $K_d$  value obtained for LukG was 2 log higher (Fig. 8B).

Although BLI has limitations in measuring very low dissociation rate constants, we wanted to investigate the contribution of the individual rate constants to the binding of the antibodies to LukGH versus LukG (not possible to measure by MSD). BLI analysis detected comparable strong binding affinity of the  $\alpha$ LukGH-mAb#5.H1H2 for the co-expressed LukGH complex and the reconstituted LukG+H complex, with measured  $K_d$  values  $\sim 2$  log lower than that measured with LukG (Fig. S7). We could not observe any binding to LukH with concentrations of up to 500 nM. The weaker binding to LukG was due to both a decrease in  $k_{on}$  and an increase in  $k_{off}$ . While the absolute equilibrium dissociation constant ( $K_d$ ) values obtained by the BLI and MSD are different, due in part to the different conditions used (e.g., temperature, biotinylated antigen in MSD vs. non-modified antigen in BLI), but also to the limited sensitivity of the BLI method,<sup>25</sup> the relative values for different antigens determined by the same method are in good agreement.

During recombinant production of LukGH we observed that the monomers, especially LukG, were more difficult to produce as soluble proteins compared to the co-expressed complex. Therefore, we wanted to confirm that lower binding to LukG

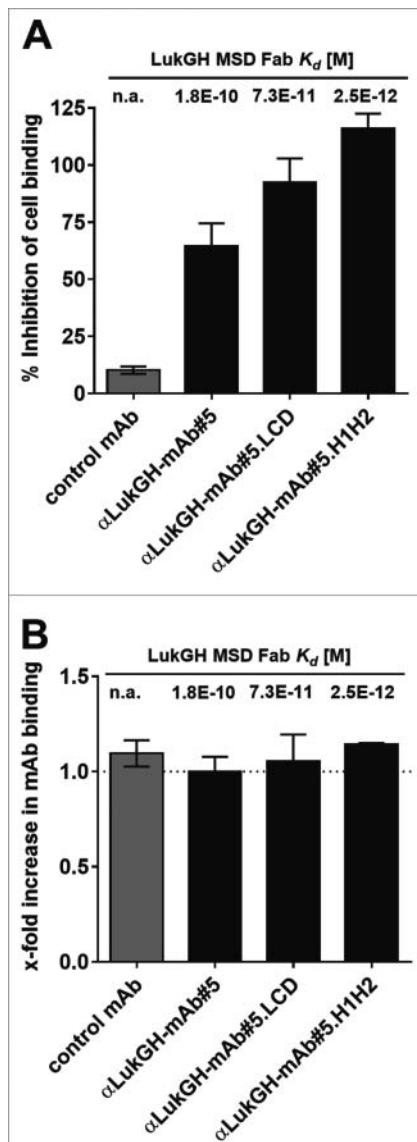


**Figure 7.** LukGH neutralizing mAbs inhibit LukGH binding to human PMNs but do not bind cell-associated toxin. (A) Biotinylated LukGH was pre-incubated with a 5-fold molar excess of indicated mAbs prior to addition of human PMNs. After a washing step to remove unbound toxin, cell-bound LukGH was quantified using a streptavidin secondary reagent by flow cytometry. (B) PMNs were incubated with LukGH on ice and stained with anti-LukGH mAbs and an Alexa Fluor 488 conjugated anti-human secondary reagent. Antibody binding is expressed as x-fold increase relative to mAb binding in absence of LukGH. Data are presented as mean  $\pm$  SEM of 2 independent experiments.

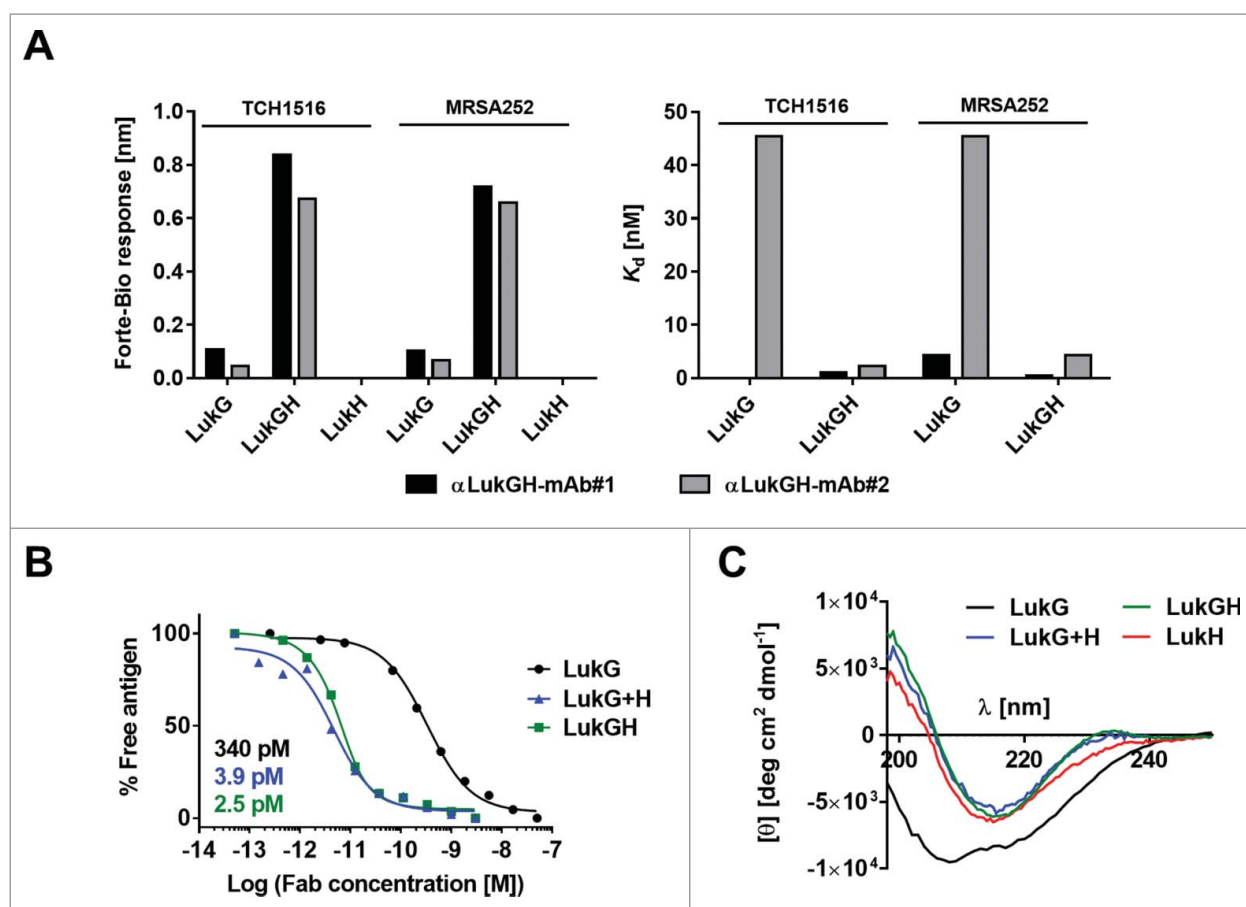


**Figure 8.** LukGH dimer selected mAbs that preferentially bind to the LukGH dimer and not to the monomers. (A) Response and  $K_d$  values of LukGH binding antibodies toward LukGH, LukG and LukH from different *S. aureus* strains determined by BLI. (B) Binding profiles of LukG, co-expressed LukGH and reconstituted LukG+H complexes for  $\alpha$ LukGH-mAb#5.H1H2 analyzed by MSD. The solid lines in (B) represent the fit of the data to a 1:1 binding model, yielding the  $K_d$  values given in the graphs. (C) Circular dichroism spectra of LukGH, LukG, LukH and LukG+H measured at 0.2–0.5 mg/ml protein, in pH 7.5 (7.9 for LukG).

was not the result of inferior protein quality. Far-UV circular dichroism (CD) revealed that the LukGH complex had a predominantly  $\beta$ -sheet structure, while LukG was partly unfolded (Fig. 8C). Importantly, the reconstituted LukG+H complex displayed a very similar CD profile to the co-expressed LukGH complex, suggesting that the secondary structure of LukG changed upon binding to LukH.

These data, together with the superior binding affinity measured with the LukGH complex, suggested that LukH induces a conformational change in LukG upon binding, which creates the high affinity binding epitope for antibody recognition.

#### Localization of the binding epitopes of LukGH-Fab by X-ray crystallography

To better understand the molecular basis of the preferential binding of antibodies to the LukGH complex over the single components, we wanted to determine the exact binding site by X-ray crystallography. We selected one of the most potent LukGH mAbs,  $\alpha$ LukGH-mAb#5.H1H2, that competed with most LukGH-dimer neutralizing antibodies, suggesting that they share the epitope binding region.

The LukGH-Fab ternary complex was purified by gel filtration, concentrated and subjected to crystallization trials. The

crystal structure was solved at 2.84 Å resolution (Table 1) and contained 2 ternary LukGH-Fab complexes in the asymmetric unit (PDB code 5K59). The Fab  $\alpha$ LukGH-mAb#5.H1H2 binds *via* the CDR in CDR R stands for region to a conformational epitope in the predicted cell-binding region of the LukGH complex on the LukG polypeptide (Fig. 9A). The interaction between  $\alpha$ LukGH-mAb#5.H1H2 and LukGH occurs in the rim domain of LukGH and involves residues from loops Gly64-Asn75, Phe199-Lys216 and Trp262-Gly269 in LukG and from both heavy and light chain CDRs in the Fab (Table 2). The buried surface area between LukG and the heavy chain is 526 Å<sup>2</sup>, and with the light chain 323 Å<sup>2</sup> (taking the average of the 2 copies in the asymmetric unit). The core of the LukG-Fab interface is formed by LukG aromatic residues (Tyr73, Trp74, Trp208 and Trp262) (Fig. 9A, Table 2). Interestingly, all residues involved in contacts were present in the naïve parent antibody ( $\alpha$ LukGH-mAb#5), except Asn30 (LC-CDR1) and Phe92 (LC-CDR3), which were selected during affinity maturation.

We previously reported the crystal structure of the LukGH octamer and identified 2 interfaces: interface 1 involved in higher-order oligomerization and interface 2 involved in heterodimer formation. The dimer in the LukGH-Fab complex has a similar arrangement to the interface 2 dimer observed in the LukGH octamer (PDB code 4TW1).<sup>12</sup> The 2 monomers in

**Table 1.** Data collection and refinement statistics for structure determination.

Data collection	
Beamline	I911-3 / MAX-II
Detector	marMosaic 225 CCD
Wavelength (Å)	1.0000
Space group	P2 <sub>1</sub>
Cell dimensions (Å)	a = 74.8, b = 160.9, c = 119.5
(°)	$\alpha = 90^\circ, \beta = 101.2^\circ, \gamma = 90^\circ$
Resolution range (Å) #	48.8–2.84 (2.91–2.84)
R <sub>merge</sub> (I) (%) #	10.8 (88.3)
Mean (I/σ(I)) #	10.1 (1.4)
Completeness (%) #	99.3 (92.5)
Multiplicity #	3.7 (3.5)
No of observed reflections #	241895 (14977)
No of unique reflections #	64655 (4262)
Refinement	
Resolution (Å)	48.8–2.84
R <sub>model</sub> (F) (%) #	19.9 (31.3)
R <sub>free</sub> (F) (%) #	23.9 (35.9)
No of unique reflections used	61207
No of non-hydrogen atoms	15764
No of protein atoms	15744
Data-to-parameter ratio	0.97
No of water molecules	4
Average B-factors (Å <sup>2</sup> )	
Protein atoms	45.8
Water molecules	33.8
Rmsd from ideal geometry	
Bond lengths(Å)	0.01
Bond angles (°)	1.39
Ramachandran plot	
Residues in favored regions	1826 (93.5%)
Residues in favored plus allowed regions	1928 (98.7%)

#Figures in parentheses are those for the highest resolution shell.

the LukGH dimer were superimposed on the monomer structures of LukF and LukS.<sup>26,27</sup> Superposition of the LukH protomer on LukS (PDB code 1T5R,<sup>27</sup> C<sub>α</sub> rmsd of 1.37 Å for 246

atoms), shows that the main differences are in the 3 loops forming the rim domain, whereas the cap domain, including the stem region, is relatively well conserved in the 2 toxins (Fig. 9B). However, when comparing LukG with LukF [PDB code 1PVL,<sup>26</sup> C<sub>α</sub> root mean square deviation (rmsd) of 1.58 Å for 258 atoms], significant differences were observed between the stem regions (C<sub>α</sub> rmsd of 10.60 Å for 33 atoms/9.97 Å for 32 atoms for LukG and LukF) compared to the S-components (0.86 Å for 33 atoms for LukH and LukS). In LukF, the stem domain is folded back against the cap domain, while in LukG, it expands outside the LukG cap region to latch onto the LukH monomer (Fig. 9B). This interface is stabilized by electrostatic interactions (Lys45 in LukH and Asp124 in LukG) and a series of polar contacts (Gly 44, Ile46, Asn163 in LukH with Phe 125, Gly123, Leu132 in LukG) and a hydrophobic core (Phe 125, Ile127, Leu132, Ile136 in LukG and Ile46, Ile69, Tyr165 in LukH), which could explain the propensity for mis-folding and aggregation of the single components, particularly LukG. In addition, there are 3 salt bridges between the rim domains of LukG and LukH, which were also observed in the LukGH octamer structure.<sup>12</sup>

## Discussion

Higher titers of anti-toxin antibodies in patients with invasive *S. aureus* disease were found to correlate with favorable disease outcome.<sup>28–30</sup> Therefore, novel immune approaches aimed at neutralizing the pore forming toxins of *S. aureus* have emerged,<sup>31,32</sup> and anti-alpha-hemolysin antibodies that showed protection in various animal models of disease are currently in clinical trials.<sup>33–35</sup> We previously described a mAb that is able to neutralize alpha-hemolysin and 4 of the 5 bi-component

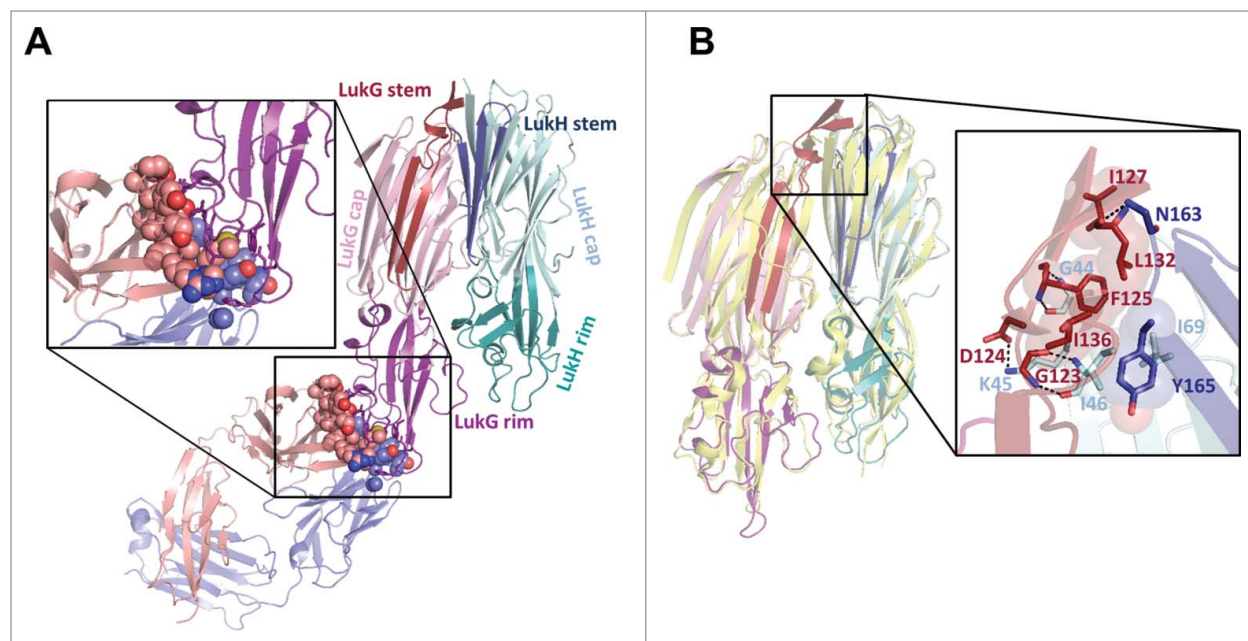


**Figure 9.** X-ray crystal structure of the LukGH- $\alpha$ LukGH-mAb#5.H1H2 Fab complex. (A) The structure of the complex formed by LukGH and the Fab of  $\alpha$ LukGH-mAb#5.H1H2 is shown as a ribbon with LukG – magenta/red, LukH – cyan/blue, and the Fab heavy chain – salmon pink and light chain – slate blue; the contact residues are shown as spheres for the Fab and sticks for LukG. (B) Overlay of the LukG and LukH (cap, stem and rim regions as represented in (A)) in the LukGH dimer with LukF (yellow, PDB code 1PVL) and LukS (yellow, PDB code 1T5R) is shown on the left. The interaction region between the LukG stem domain and LukH, with interacting residues represented as sticks/spheres and the polar contacts as dotted lines, is shown on the right.



**Table 2.** Contact residues in the LukGH-Fab ( $\alpha$ LukGH-mAb#5.H1H2) interface.

CDR	Fab residue	LukG residue
HC-CDR1	Ser33	Asn206, Leu207
	Tyr35	Leu207, Trp208, Asp211
HC-CDR2	Asn52	Trp208
	Tyr54	Leu207, Asp211
	Ser56	Asp211
	Ser58	Lys210, Asp211
	Thr59	Asn71
	Tyr60	Asn71, Trp208
HC-CDR3	Glu100	Trp208
	Arg101	Asn206
	Gly102	Asn206
	Met103	Tyr73, Tyr74, Asn206, Trp262
	His104	Asn206, Phe267
LC-CDR1	Asn30 (LCD) #	Arg264
	Tyr32	Trp74, Trp262, Arg264
LC-CDR2	Ala50	Phe267
LC-CDR3	Gln91	Tyr73, Trp74
	Phe92 (LCD) #	Tyr73, Trp74, Arg264
	Pro94	Tyr73, Trp208
	Phe96	Tyr73, Trp208

#Residue introduced during LCD affinity maturation.

toxins of *S. aureus*: gamma-hemolysin AB and CB, LukSF and LukED. This antibody also displayed potent *in vitro* activity toward human cells, and significant efficacy in models of *S. aureus* pneumonia and sepsis.<sup>35</sup>

The aim of this study was to isolate human mAbs able to neutralize the fifth leukocidin, LukGH (LukAB), one of the most potent cytotoxins of *S. aureus* and therefore expected to significantly contribute to immune evasion. We employed a high diversity library of full-length human IgG1s presented on the surface of yeast cells and initially used individually expressed LukG and LukH monomers in the selections. Although these selections yielded good binders with  $K_d$  values of 0.7 to 50 nM, particularly for LukG, no LukGH neutralizing activity was detected for these mAbs. These findings were in contrast to our previous experience with other bi-component toxin monomers using the same mAb discovery platform.<sup>35</sup> This prompted us to investigate the possibility that LukG and LukH interact in solution in a way that may prevent antibody binding. Sequential mixing experiments of the individual toxins and the mAbs proved this hypothesis. This observation led to the discovery that LukG and LukH, unlike the other 4 bi-component leukocidins of *S. aureus*, interact in solution, and form dimers before target cell binding.<sup>12</sup> While we performed these studies, DuMont et al reported the co-purification of LukG and LukH from *S. aureus* culture supernatant and suggested complex formation by the monomers.<sup>13</sup>

When we repeated the mAb selections using the co-expressed recombinant LukGH heterodimer as bait, we were able to identify potent neutralizing mAbs active against both the recombinant forms of the leukocidin and bacterial supernatants. These antibodies displayed detectable binding either to LukG (F-component) or LukH (S-component), some to both. Interestingly, LukH binders were weaker neutralizers, which is in line with our observations from previous studies with the other bi-component leukocidins, where selection with F-components (HlgB, LukD, LukF) resulted in more potent antibodies than with S-components (HlgA, HlgC, Luke, LukS).<sup>35</sup> Moreover, LukG-binders were more cross-reactive and cross-

neutralizing between different sequence variants of LukGH. To our knowledge, this is the first report describing neutralizing mAbs against LukGH. These data indicate that native conformation of LukGH is essential to generate high affinity, neutralizing mAbs.

Successive screening with light chain diversified and heavy chain CDR1 and/or CDR2 mutated sub-libraries resulted in LukGH mAbs with  $K_d$  values in the single digit picomolar range. The increase in affinity correlated very well with increased potency in cell-based toxin-neutralization assays.

We found that the neutralizing mAbs exerted their effect by interfering with LukGH binding to the target cells. The crystal structure of the LukGH-Fab complex (generated with one of the most potent LukGH cross-neutralizing mAbs) confirmed that the epitope is located in the predicted cell binding region of LukGH. BLI detected weak binding (low response units) of LukG to mAb-coated tips, but tight binding of LukGH. No binding was detectable with the LukH monomer. Based on MSD measurements, the most potent mAb bound LukGH in the single digit picomolar range, while the affinity to LukG was ~100 fold lower. We concluded that the difference in affinities was due to the different conformation of the epitope, mainly located in LukG, when not in complex with LukH. This was confirmed by CD analysis of the single components and the complex, the latter showing a lower degree of unstructured regions. When the LukG and LukH monomers were mixed and purified, the complex obtained had virtually the same affinity for the most potent mAb as the co-expressed LukGH complex. This indicates an interaction-induced folding of LukGH, which is supported by extensive interactions between the stem and rim regions of the 2 polypeptides in the complex, which are unique to LukGH, as observed in the crystal structure of the dimer.

*S. aureus* strains express up to 5 leukocidins. Therefore, full protection of phagocytic cells requires neutralization of all 5 leukocidins. This can be achieved by combining the broadly toxin cross-neutralizing human mAb (ASN-1) discovered by the same technology as used in this study and reported previously,<sup>35</sup> and a LukGH neutralizing mAb described in this study (ASN-2). Such a mAb combination (ASN100) completed Phase 1 clinical testing for safety and is aimed at prophylaxis and therapy of severe *S. aureus* infections.

## Materials and methods

### Bacterial strains, culture supernatants

The *S. aureus* USA300 strain TCH1516 (ATCC® BAA-1717™) was obtained from ATCC (Manassas, VA). Isogenic mutants lacking the *hla*, *lukED*, *lukSF*, *hlgABC* and *lukGH* genes were generated in the TCH1516 background by homologous recombination based on previously published methods.<sup>35,36</sup> To generate multiple gene deletion mutants, competent cells were prepared in the corresponding mutant strains. Bacterial culture supernatants (CS) were prepared in RPMI-1640 (Gibco #32404-014) supplemented with 1% of casamino acids (Amresco, #J851) (RPMI-CAS). Bacteria were grown from a single colony to stationary phase in 20 ml medium at 37°C shaking at 200 rpm. CS were harvested by culture

centrifugation at 5000 x g, followed by filter sterilization of the supernatant using 0.1  $\mu$ m pore size syringe filters (Millipore, #SLVV033RS).

### Human target cells

Cell-based assays were performed using either human PMNs or “neutrophil-like” differentiated HL-60 promyelotic leukemia cells. PMNs were isolated from heparinized human whole blood, either obtained from healthy volunteers or from the Austrian Red Cross. Cells were purified using Percoll (Percoll Plus, GE Healthcare, #17-5445-01) gradient centrifugation as described in Badarau et al.<sup>12</sup> HL-60 cells (ATCC CCL-240<sup>TM</sup>) were cultured in RPMI-1640 culture medium supplemented with 10% FCS (Sigma, #F7524), L-Glutamine (Invitrogen, #25030-024), and Penicillin-Streptomycin (Gibco, #15140-122), referred to as “neutrophil medium” and differentiated with N,N-dimethylformamide (Fisher BioReagents, #BP1160-500) at 100 mM for 3–5 d as described elsewhere.<sup>12,37</sup>

### In vitro assays to measure toxin mediated cell lysis

Either primary human PMNs or differentiated HL-60 cells were used for measuring cell lysis induced by recombinant toxins or *S. aureus* culture supernatants.

Toxin activity of recombinant bi-component toxins or filter-sterilized culture supernatants was assessed by measuring cellular ATP levels. Briefly, an equimolar mixture of the F- and S- components, the co-expressed LukGH complex or the culture supernatant was serially diluted in neutrophil medium and used for intoxication of  $2.5 \times 10^4$  cells for 4 h at 37°C at 5% CO<sub>2</sub> in 96-well, half-area luminescent plates (Greiner #675083). Cell viability was then measured using the Cell Titer-Glo<sup>®</sup> Luminescent Cell Viability Assay Kit (Promega, #G7573) according to the manufacturer’s instructions. Percent viability was calculated relative to mock-treated cells incubated in neutrophil medium (100% viability).

### Isolation of LukG, LukH and LukGH complexes

Recombinant LukG and LukH monomers and LukGH complexes were generated based on genome sequences of the *S. aureus* strains TCH1516 (USA300 CA-MRSA), MRSA252 (CC30, ST36), MSHR1132 (“silver *S. aureus*) and H19 (live-stock-derived CC10) and produced in *E. coli* Tuner DE3 as described previously.<sup>12</sup> Briefly, LukG and LukH were isolated from inclusion bodies, solubilized in 8 M urea (Roth, #2317.2), purified by ion exchange and size-exclusion chromatography (SEC) and formulated in 20 mM 3-(cyclohexylamino)-1-propanesulfonic acid (CAPS, Sigma Aldrich, #C2632), pH 10.2 plus 500 mM NaCl (Fisher Scientific, #BP358-10) for LukG and 50 mM sodium phosphate (Fisher Scientific, #BP332-1, BP329-1), pH 7.5, 500 mM NaCl for LukH. The LukGH complexes were obtained by co-expressing LukG and LukH in the same *E. coli* cell, in soluble form, and purified by metal ion affinity (LukG contains a NusA/His<sub>6</sub> tag at the N-terminus) followed by tag cleavage and cation exchange chromatography.

Native LukGH from the *S. aureus* strain Newmann was isolated from the culture supernatant of an overnight culture

grown at 37°C for 16 h in RPMI supplemented with 1% casamino acids and 0.4 mM of the iron-chelator 4,4'-dipyridyl (Acros Organics, #117500250). The cleared culture supernatant was concentrated 100-fold and 5 mL of the concentrated supernatant was incubated with 0.5 mg of a specific anti-LukGH human mAb for 30 min at room temperature. The antibody-antigen complex was then captured on anti-human CH1 beads (Capture Select, Life Technologies, #19432001L), and after washing with phosphate-buffered saline (PBS), pH 7.2 (Gibco, #14190-160), the antigen was eluted with 20 mM sodium acetate (Sigma # 55636), pH 4.0 with 150 mM NaCl. The fractions containing LukGH were neutralized with 10% of 1 M Tris pH 8.0 (Ambion, #AM9856), diluted with water to a final NaCl concentration of 50 mM and further purified by cation exchange chromatography as described for the recombinant LukGH complex.<sup>12</sup> Isolated Newmann LukGH was more than 95% pure based on SDS-PAGE analysis. Protein integrity was also verified by ESI-MS (Bruker Maxis 4G).

### Determination of LukGH neutralizing activity of antibodies

For neutralization assays with mAbs, antibodies were serially diluted in neutrophil medium and mixed with recombinant toxins or sterile-filtered culture supernatants at a fixed concentration as indicated in the figure legends. Luminescent cell viability assays (described above) were started after a 30 min pre-incubation step to allow antibody-toxin binding. Percent inhibition of toxin activity was calculated using the following formula: % inhibition = [(normal activity - inhibited activity) / (normal activity)] x 100. A human IgG1 control mAb expressed by yeast cells and generated against an irrelevant antigen was included in all assays. Data were analyzed by non-linear regression analysis using GraphPad Prism 6 (GraphPad).

### PMN infection assays with live bacteria

Overnight cultures of *S. aureus* grown in RPMI-CAS were freshly diluted 1:100 and grown to mid-log phase (OD<sub>600</sub>: 0.5) at 37°C, with shaking at 200 rpm. Bacteria were harvested by centrifugation (5 min, 5000 g, 4°C), washed in PBS pH 7.2 to remove secreted toxin and re-suspended in assay buffer (RPMI-1640 + 10% FCS + 2 mM L-glutamine + 10 mM HEPES (PAA, #2003,6500)) at  $2 \times 10^8$  CFU/ml for infection at MOI 100.

Bacteria were then further diluted for infection at different MOIs in assay medium and transferred to 96-well, half-area plates (Greiner, #675083) in 12.5  $\mu$ l volumes, mixed with antibodies (in 12.5  $\mu$ l) and  $2.5 \times 10^4$  human PMNs/well (12.5  $\mu$ l). To ensure comparable input CFUs when working with different bacterial strains, dilutions used in the assays were subjected to a parallel measurement of microbial viability in a BacTiter-Glo<sup>TM</sup> Microbial Cell Viability Assay (Promega, #G8232) according to the manufacturer’s instructions.

The mixture of antibodies, bacteria and PMNs was incubated for 90 min at 37°C and 5% CO<sub>2</sub>, followed by addition of 12.5  $\mu$ l Calcein-AM fluorescent viability dye (eBioscience, # 65-0853-39) at a final concentration of 4  $\mu$ M. The total reaction was further incubated for 30 min to allow dye hydrolysis and development of a fluorescent signal. PMN cell viability was

then quantified using a fluorescence plate reader with excitation at 485 nm and emission at 528 nm. Percent viability was calculated relative to mock-treated cells incubated in the same medium (100% viability).

### Isolation of LukG, LukH and LukGH binding human mAbs

As a source of mAbs, a library of yeast cells engineered to express full-length human IgG1 antibodies was employed. This yeast library reflects the natural pre-immune repertoire created by the human immune system and is based on rational design informed by analysis of publicly available databases of human antibody sequences. In particular, 20 VH and 9 VK germlines, corresponding to those among the most highly expressed in humans, were chosen as scaffolds for CDR-H3 and CDR-L3 diversities. CDR-H3 diversity was generated through combinatorial pairing of selected human V (AR or AK portion) D, and J segments, while CDR-L3 diversity was built from V-J combinations. Specific germline and other segment choices as well as other details are described by Vasquez et al.<sup>23</sup> Toxin-binding mAbs were identified by incubating biotin labeled LukH, LukG or LukGH-dimer at different concentrations with antibody-expressing yeast cells followed by magnetic bead selection and fluorescence-activated cell sorting employing streptavidin secondary reagents in several successive selection rounds. Antibodies were then produced by the selected yeast clones and purified by Protein A affinity chromatography. Selected mAbs were further affinity matured by light chain diversification (LCD) and heavy chain CDR1 and/or CDR2 mutagenesis (H1H2) as described previously.<sup>38</sup>

Binding of mAbs to the different toxins was confirmed by interferometry measurements using a fortéBIO Octet Red instrument (Pall Life Sciences). The biotinylated antigen or the antibody was immobilized on the sensor and the association and dissociation of the antibody Fab or of the antigen, respectively (typically 200 nM), in solution [(PBS, pH 7.4) + 1% bovine serum albumin (BSA, Sigma, #S0876)], were measured.

### Generation of purified antibodies

Antibodies derived from the yeast library were produced by selected yeast clones, and for  $\alpha$ LukGH-mAb#5.H1H2 also by CHO-3E7 cells (Biotechnology Research Institute, Canada), transiently transfected with vector plasmids encoding human antibody (IgG1) heavy and light chains using mammalian expression vectors pTT5 (Biotechnology Research Institute, Canada) using PEI MAX<sup>TM</sup> transfection reagent (Polysciences). Yeast-produced antibodies were used in screening and cell-based *in vitro* experiments, unless otherwise stated. Affinity measurements for  $\alpha$ LukGH-mAb#5.H1H2 were performed using the mAbs produced in CHO-3E7 cells. Supernatants were harvested 8 d after transfection and IgGs were purified by Protein A affinity chromatography (HiTrap MabSelect, GE Healthcare, #28-4082-56), by eluting with 100 mM sodium acetate, pH 3.5 followed by neutralization and dialysis in PBS pH 7.2. Antibody purity and monomer content (> 95%) were estimated based on SDS-PAGE and SEC analysis and concentrations were determined from the absorption at 280 nm. Negative control mAbs used in this study were generated in

the same expression system as the anti-toxin mAbs and either raised against hen egg-white lysozyme (control mAb for yeast produced mAbs) or against the F-protein of respiratory syncytial virus (motavizumab, used as a control for CHO-expressed mAbs).

Mouse polyclonal antibodies were generated against recombinant LukG and LukH. Female, 6–8 week old BALB/cJRj mice (JanvierLabs, France) were subcutaneously boosted 3 times with 10  $\mu$ g of toxin per animal, formulated in Freund's adjuvant. IgGs were purified from hyper-immune and the respective pre-immune sera *via* Protein G affinity chromatography (Protein G Sepharose, GE Healthcare, #17-0618-01), by eluting with 100 mM glycine pH 2.0, followed by neutralization and dialysis in 25 mM HEPES, pH 7.3, 150 mM NaCl.

### Flow cytometry-based toxin binding assays

For toxin binding inhibition assays, biotinylated co-expressed LukGH at 27.3 nM concentration was pre-incubated with a 5-fold molar excess of mAbs for 30 min at room temperature in HBSS (Gibco) + 0.5% BSA (Biomol, #01400.1), prior to incubation with  $1 \times 10^6$  PMNs for 30 min on ice. After washing the cells in HBSS, cell-bound toxin was detected with Alexa Fluor 488-labeled streptavidin (Molecular Probes, #S32354), and analyzed by flow cytometry using an iCyt Eclipse flow cytometer (Sony Biotechnology Inc.). Data were analyzed using the FCS Express software version 4 (De Novo Software). Binding was expressed as median fluorescent intensity. mAb based binding inhibition was calculated based on median fluorescent intensities using the following formula: % inhibition = [(normal activity - inhibited activity) / (normal activity)] x 100.

To test mAb binding to cell-associated toxin, PMNs were incubated with 1.37 nM (a typically lethal concentration used in neutralizations assays) of biotinylated co-expressed LukGH for 30 min on ice. Toxin binding to the PMNs was confirmed as described above and cells were stained with anti-LukGH mAbs (at 33.3 nM) and Alexa Fluor 488-labeled goat anti-human IgG secondary reagent (Jackson ImmunoResearch, #109-546-097). MAb binding in presence of toxin is expressed as the increase relative to the binding signal of the same antibody in the absence of toxin. Samples stained with secondary reagent only (staining control) and cells incubated with toxin and negative control antibody were included in all experiments.

### Interferometry and MSD-based binding assays

Binding of mAbs to the LukG, LukH and LukGH variants was measured by BLI using a fortéBIO Octet Red instrument (Pall Life Sciences). The antibody (10  $\mu$ g/ml) was immobilized on the AHC (anti-human capture) sensor (Pall Life Sciences, #18-5063) to give a sensor loading of  $\sim$ 1.2 nm. The association of the antigen (100 nM), in solution [PBS, pH 7.2 plus 3% BSA (for the naïve mAbs) or 1% BSA (for the affinity mature mAbs)], at 30°C was monitored for 300 s (for the naïve mAbs) and 600 s (for the affinity mature mAbs). The sensors were then immersed in the same buffer, for 180 s (for the naïve mAbs) or 1800 s (for the affinity mature mAbs) to monitor the dissociation of the antigen. Response values after completion of the association phase were determined using the fortéBIO

Analysis Software version 7.0; for the naïve mAbs the response values were corrected by subtracting the corresponding value of a negative control mAb. For response values above 0.05 nm, kinetic rate constants ( $k_{\text{on}}$  and  $k_{\text{off}}$ ) were determined for each progress curve by fitting simultaneously the association and dissociation phases to a 1:1 binding model and the dissociation constants ( $K_d$  values) were calculated as  $k_{\text{off}}/k_{\text{on}}$ . Fab  $K_d$  affinities were measured by the MSD-SET method using a Sector Imager 2400 instrument (Meso Scale Discovery). Typically, 15–100 pM of biotinylated antigen was incubated with Fab (generated by papain digestion) at various concentrations; this mixture was allowed to come to equilibrium for 16 h at room temperature, and unbound antigen was captured by IgG immobilized on a 96-well Standard MSD plate (Meso Scale Discovery, #L15XA). The antigen was then detected using 250 ng/mL Streptavidin-sulfotag reagent (Meso Scale Discovery, #R32AD-5), and resultant signals were normalized and plotted as a function of Fab concentration in GraphPad Prism 6. The data were fit using a quadratic equation in GraphPad Prism to extract the dissociation constant ( $K_d$ ).<sup>25</sup> Several antibodies with sub-picomolar affinity reached the lower limit of affinity measurement by MSD.

The interference of LukH with the binding of a LukG-specific antibody to LukG was determined in BLI in a set-up similar to that described above. The antibody (10  $\mu\text{g/ml}$ ) was immobilized onto AHC sensors and the binding of LukG (200 nM) pre-incubated for 10 min at 30°C with LukH at different concentrations (0 – 600 nM), in solution (PBS, pH 7.2 + 1% BSA), was monitored for 300 s; dissociation in the same buffer was monitored for 180 s. The response and the calculated  $k_{\text{on}}$  values, determined as described above, were plotted as a function of LukH molar equivalents ( $[\text{LukH}]/[\text{LukG}]$ ).

### Circular dichroism

Far UV (195–250 nm) CD spectra were recorded on a Chirascan (Applied Photophysics) spectrometer in a 0.5 mm cuvette (Applied Photophysics), at 20°C, at protein concentrations between 0.1 and 0.3 mg/ml in 20 mM sodium phosphate buffer pH 7.5 with 200 mM NaCl for the LukGH and LukG+H complexes; 50 mM sodium phosphate buffer pH 7.5 with 500 mM NaCl for LukH; and 20 mM CAPS, 56 mM Tris (Sigma-Aldrich, #252859) pH 7.9 with 500 mM NaCl for LukG.

### Preparation of reconstituted LukG+H complex

Individually expressed and purified LukG (formulated in 25 mM CAPS, pH 10.0 plus 500 mM NaCl) and LukH (formulated in 50 mM phosphate, pH 7.5 plus 500 mM NaCl) single components were concentrated to  $\sim 1$  mg/ml, and each protein was diluted with 20 mM HEPES pH 7.5 to a final NaCl concentration of 250 mM. The 2 proteins were then mixed in equimolar amounts and further diluted with water to give a final salt concentration of 125 mM. The mixture was then purified by cation exchange chromatography as previously described for the co-expressed complex, to give the reconstituted LukG+H complex.<sup>12</sup>

### Protein crystallization, data collection, structure determination and refinement

Co-purified LukGH\_TCH1516 produced as described previously<sup>12</sup> was mixed in a 1:1.5 molar ratio with the Fab of  $\alpha\text{LukGH-mAb}\#5.\text{H1H2}$  expressed as Fab in CHO cells and purified by LC-kappa affinity chromatography (CaptureSelect, Thermo Scientific, #083310). The mixture was concentrated, and the ternary complex isolated by SEC on Superdex 200 10/300 GL (GE Healthcare, #17-5175-01) equilibrated in 20 mM HEPES, pH 7.5, 300 mM NaCl. The fractions of the peak corresponding to the ternary Fab-LukGH complex, (as judged from the calculated molecular weight based on SEC elution volume), were diluted with 20 mM HEPES, pH 7.5, to give a final NaCl concentration of 100 mM, and concentrated to a final concentration of 17 mg/ml complex in 20 mM HEPES, pH 7.5, 100 mM NaCl.

Diffraction quality crystals were obtained using sitting drop vapor diffusion and seeding at 20°C, in a drop containing 200 nl Fab-LukGH at 1:1 ratio in 50 nl seed solution + 150 nl reservoir solution [0.3 M NaCl, 26% polyethylene glycol (PEG) 8000, 0.1 M phosphate citrate pH 4.2]. The seed solution was obtained from a condition containing 40% PEG 300, 0.1 M phosphate-citrate pH 4.2, 0.3 M NaCl, 20 mM HEPES pH 7.5. The crystal was harvested from the crystallization drop using a nylon loop, soaked briefly in a cryoprotectant solution consisting of 25% PEG 8000 (Fluka, #89510), 0.1 M phosphate-citrate pH 4.2, 0.3 M NaCl and 20% PEG 300 (Sigma, #90878) and frozen directly in liquid nitrogen. Data were collected to 2.84 Å resolution at 100 K at station I911-3 ( $\lambda = 1.0$  Å), Lund, Sweden,<sup>39</sup> equipped with a MarMosaic 225 nm detector. Diffraction images ( $n = 365$ ) were collected with an exposure time of 6 s and an oscillation range of 0.5° per image. The data were integrated using XDS<sup>40</sup> and scaled using AIMLESS.<sup>41</sup> The space group was P21. The CCP4 suite was used to solve and refine the structure of Fab-LukGH.<sup>42</sup> The solvent content and Matthews' coefficient were calculated to be 58.4% and 2.96, respectively, which corresponds to 2 Fab-LukGH complexes in the asymmetric unit. The structure was determined by molecular replacement using Phaser.<sup>43</sup> The dimer between chains B and C from previously solved LukGH and the heavy and light chains of a Fab from a Fab-Hla complex (unpublished data) were used as search models. Phaser found 2 LukGH molecules and 2 Fab molecules. After molecular replacement, rigid body refinement was done in Refmac5.<sup>44</sup> Several cycles of refinement of the coordinates using the program Refmac5 were combined with manual rebuilding using Coot and followed by a final step of TLS refinement.<sup>45,46</sup> The structure quality was analyzed using MolProbity.<sup>47</sup> Protein interfaces were analyzed with PISA<sup>48</sup> and the contact residues and the protein figures were obtained with PyMOL (The PyMOL Molecular Graphics System, Version 1.2r3pre, Schrödinger, LLC).

### Disclosure of potential conflicts of interest

The authors declare potential conflict of interest being employees of the 3 biotechnology companies involved in this research work.

## Acknowledgments

We thank Yingda Xu for technical assistance in the antibody discovery, David Hoffmann, Katharina Havlicek, Nikolina Trstenjak, Thomas Keller, Jakub Zmajkovic and Sabine Maier for technical help in antibody and LukGH expression, purification and characterization. Yeast expressed IgG material was generated and analyzed by the Molecular Core, High Throughput Expression and Analytical Group of Adimab. We also thank Christine Power for the critical reading of the manuscript.

## Funding

This work was supported by the “Basisprogramm” grants (No: 832915, 837128 and 841918) from the Austrian Research Promotion Agency (FFG), awarded to Arsanis Biosciences GmbH.

## References

- Rigby KM, DeLeo FR. Neutrophils in innate host defense against *Staphylococcus aureus* infections. *Semin Immunopathol* 2012; 34:237-59; PMID:22080185; <http://dx.doi.org/10.1007/s00281-011-0295-3>
- Spaan AN, Surewaard BG, Nijland R, van Strijp JA. Neutrophils versus *Staphylococcus aureus*: a biological tug of war. *Annu Rev Microbiol* 2013; 67:629-50; PMID:23834243; <http://dx.doi.org/10.1146/annurev-micro-092412-155746>
- Vandenesch F, Lina G, Henry T. *Staphylococcus aureus* hemolysins, bi-component leukocidins, and cytolytic peptides: a redundant arsenal of membrane-damaging virulence factors? *Front Cell Infect Microbiol* 2012; 2:12; PMID:22919604; <http://dx.doi.org/10.3389/fcimb.2012.00012>
- Alonzo F, Torres VJ. The bicomponent pore-forming leucocidins of *Staphylococcus aureus*. *Microbiol Mol Biol Rev MMBR* 2014; 78:199-230; PMID:24847020; <http://dx.doi.org/10.1128/MMBR.00055-13>
- Panton P, Valentine F. Staphylococcal toxin. *Lancet* 1932; 219:506-8; [http://dx.doi.org/10.1016/S0140-6736\(01\)24468-7](http://dx.doi.org/10.1016/S0140-6736(01)24468-7)
- Jayasinghe L, Bayley H. The leukocidin pore: evidence for an octamer with four LukF subunits and four LukS subunits alternating around a central axis. *Protein Sci Publ Protein Soc* 2005; 14:2550-61; PMID:16195546; <http://dx.doi.org/10.1110/ps.051648505>
- Miles G, Movileanu L, Bayley H. Subunit composition of a bicomponent toxin: staphylococcal leukocidin forms an octameric transmembrane pore. *Protein Sci Publ Protein Soc* 2002; 11:894-902; PMID:11910032; <http://dx.doi.org/10.1110/ps.4360102>
- Yamashita K, Kawai Y, Tanaka Y, Hirano N, Kaneko J, Tomita N, Ohta M, Kamio Y, Yao M, Tanaka I. Crystal structure of the octameric pore of staphylococcal  $\gamma$ -hemolysin reveals the  $\beta$ -barrel pore formation mechanism by two components. *Proc Natl Acad Sci U S A* 2011; 108:17314-9; PMID:21969538; <http://dx.doi.org/10.1073/pnas.1110402108>
- Colin DA, Mazurier I, Sire S, Finck-Barbançon V. Interaction of the two components of leukocidin from *Staphylococcus aureus* with human polymorphonuclear leukocyte membranes: sequential binding and subsequent activation. *Infect Immun* 1994; 62:3184-8; PMID:8039887
- Ventura CL, Malachowa N, Hammer CH, Nardone GA, Robinson MA, Kobayashi SD, DeLeo FR. Identification of a novel *Staphylococcus aureus* two-component leukotoxin using cell surface proteomics. *PLoS One* 2010; 5:e11634; PMID:20661294; <http://dx.doi.org/10.1371/journal.pone.0011634>
- Dumont AL, Nygaard TK, Watkins RL, Smith A, Kozhaya L, Kreiswirth BN, Shopsin B, Unutmaz D, Voyich JM, Torres VJ. Characterization of a new cytotoxin that contributes to *Staphylococcus aureus* pathogenesis. *Mol Microbiol* 2011; 79:814-25; PMID:21255120; <http://dx.doi.org/10.1111/j.1365-2958.2010.07490.x>
- Badarau A, Rouha H, Malafa S, Logan DT, Håkansson M, Stulik L, Dolezilkova I, Teubenbacher A, Gross K, Maierhofer B, et al. Structure-function analysis of heterodimer formation, oligomerization, and receptor binding of the *Staphylococcus aureus* bi-component toxin LukGH. *J Biol Chem* 2015; 290:142-56; PMID:25371205; <http://dx.doi.org/10.1074/jbc.M114.598110>
- DuMont AL, Yoong P, Liu X, Day CJ, Chumbler NM, James DB, Alonzo F, Bode NJ, Lacy DB, Jennings MP, et al. Identification of a crucial residue required for *Staphylococcus aureus* LukAB cytotoxicity and receptor recognition. *Infect Immun* 2014; 82:1268-76; PMID:24379286; <http://dx.doi.org/10.1128/IAI.01444-13>
- Spaan AN, Vrieling M, Wallet P, Badiou C, Reyes-Robles T, Ohneck EA, Benito Y, de Haas CJ, Day CJ, Jennings MP, et al. The staphylococcal toxins  $\gamma$ -haemolysin AB and CB differentially target phagocytes by employing specific chemokine receptors. *Nat Commun* 2014; 5:5438; PMID:25384670; <http://dx.doi.org/10.1038/ncomms6438>
- Spaan AN, Henry T, van Rooijen WJ, Perret M, Badiou C, Aerts PC, Kemmink J, de Haas CJ, van Kessel KP, Vandenesch F, et al. The staphylococcal toxin Pantone-Valentine Leukocidin targets human C5a receptors. *Cell Host Microbe* 2013; 13:584-94; PMID:23684309; <http://dx.doi.org/10.1016/j.chom.2013.04.006>
- Reyes-Robles T, Alonzo F, Kozhaya L, Lacy DB, Unutmaz D, Torres VJ. *Staphylococcus aureus* Leukotoxin ED targets the chemokine receptors CXCR1 and CXCR2 to kill leukocytes and promote infection. *Cell Host Microbe* 2013; 14:453-9; PMID:24139401; <http://dx.doi.org/10.1016/j.chom.2013.09.005>
- DuMont AL, Yoong P, Day CJ, Alonzo F, McDonald WH, Jennings MP, Torres VJ. *Staphylococcus aureus* LukAB cytotoxin kills human neutrophils by targeting the CD11b subunit of the integrin Mac-1. *Proc Natl Acad Sci U S A* 2013; 110:10794-9; PMID:23754403; <http://dx.doi.org/10.1073/pnas.1305121110>
- DuMont AL, Yoong P, Surewaard BG, Benson MA, Nijland R, van Strijp JA, Torres VJ. *Staphylococcus aureus* elaborates leukocidin AB to mediate escape from within human neutrophils. *Infect Immun* 2013; 81:1830-41; PMID:23509138; <http://dx.doi.org/10.1128/IAI.00095-13>
- Malachowa N, Kobayashi SD, Braughton KR, Whitney AR, Parnell MJ, Gardner DJ, Deleo FR. *Staphylococcus aureus* leukotoxin GH promotes inflammation. *J Infect Dis* 2012; 206:1185-93; PMID:22872735; <http://dx.doi.org/10.1093/infdis/jis495>
- Boder ET, Wittrup KD. Yeast surface display for screening combinatorial polypeptide libraries. *Nat Biotechnol* 1997; 15:553-7; PMID:9181578; <http://dx.doi.org/10.1038/nbt0697-553>
- Blaise L, Wehnert A, Steukers MP, van den Beucken T, Hoogenboom HR, Hufton SE. Construction and diversification of yeast cell surface displayed libraries by yeast mating: application to the affinity maturation of Fab antibody fragments. *Gene* 2004; 342:211-8; PMID:15527980; <http://dx.doi.org/10.1016/j.gene.2004.08.014>
- Rakestraw JA, Aird D, Aha PM, Baynes BM, Lipovsek D. Secretion-and-capture cell-surface display for selection of target-binding proteins. *Protein Eng Des Sel PEDS* 2011; 24:525-30; PMID:21402751; <http://dx.doi.org/10.1093/protein/gzr008>
- Vasquez M, Feldhaus M, Gerngross T, Wittrup K. Rationally designed, synthetic antibody libraries and uses therefor; Patent No US8691730
- Xu Y, Roach W, Sun T, Jain T, Prinz B, Yu TY, Torrey J, Thomas J, Bobrowicz P, Vásquez M, et al. Addressing polyspecificity of antibodies selected from an in vitro yeast presentation system: a FACS-based, high-throughput selection and analytical tool. *Protein Eng Des Sel PEDS* 2013; 26:663-70; PMID:24046438; <http://dx.doi.org/10.1093/protein/gzt047>
- Estep P, Reid F, Nauman C, Liu Y, Sun T, Sun J, Xu Y. High throughput solution-based measurement of antibody-antigen affinity and epitope binning. *Mabs* 2013; 5:270-8; PMID:23575269; <http://dx.doi.org/10.4161/mabs.23049>
- Pédelaçq JD, Maveyraud L, Prévost G, Baba-Moussa L, González A, Courcelle E, Shepard W, Monteil H, Samama JP, Mourey L. The structure of a *Staphylococcus aureus* leucocidin component (LukF-PV) reveals the fold of the water-soluble species of a family of transmembrane pore-forming toxins. *Struct Lond Engl* 1999; 7:277-87; PMID:10368297
- Guillet V, Roblin P, Werner S, Coraiola M, Menestrina G, Monteil H, Prévost G, Mourey L. Crystal structure of leucotoxin S component:

- new insight into the Staphylococcal  $\beta$ -barrel pore-forming toxins. *J Biol Chem* 2004; 279:41028-37; PMID:15262988; <http://dx.doi.org/10.1074/jbc.M406904200>
28. Thomsen IP, Dumont AL, James DB, Yoong P, Saville BR, Soper N, Torres VJ, Creech CB. Children with invasive *Staphylococcus aureus* disease exhibit a potentially neutralizing antibody response to the cytotoxin LukAB. *Infect Immun* 2014; 82:1234-42; PMID:24379282; <http://dx.doi.org/10.1128/IAI.01558-13>
  29. Fritz SA, Tiemann KM, Hogan PG, Epplin EK, Rodriguez M, Al-Zubeidi DN, Bubeck Wardenburg J, Hunstad DA. A serologic correlate of protective immunity against community-onset *Staphylococcus aureus* infection. *Clin Infect Dis Off Publ Infect Dis Soc Am* 2013; 56:1554-61; PMID:23446627; <http://dx.doi.org/10.1093/cid/cit123>
  30. Adhikari RP, Ajao AO, Aman MJ, Karauzum H, Sarwar J, Lydecker AD, Johnson JK, Nguyen C, Chen WH, Roghmann MC. Lower antibody levels to *Staphylococcus aureus* exotoxins are associated with sepsis in hospitalized adults with invasive *S. aureus* infections. *J Infect Dis* 2012; 206:915-23; PMID:22807524; <http://dx.doi.org/10.1093/infdis/jis462>
  31. Oleksiewicz MB, Nagy G, Nagy E. Anti-bacterial monoclonal antibodies: back to the future? *Arch Biochem Biophys* 2012; 526:124-31; PMID:22705202; <http://dx.doi.org/10.1016/j.abb.2012.06.001>
  32. Cheung GY, Otto M. The potential use of toxin antibodies as a strategy for controlling acute *Staphylococcus aureus* infections. *Expert Opin Ther Targets* 2012; 16:601-12; PMID:22530584; <http://dx.doi.org/10.1517/14728222.2012.682573>
  33. Oganessian V, Peng L, Damschroder MM, Cheng L, Sadowska A, Tkaczyk C, Sellman BR, Wu H, Dall'Acqua WF. Mechanisms of neutralization of a human anti- $\alpha$ -toxin antibody. *J Biol Chem* 2014; 289:29874-80; PMID:25210036; <http://dx.doi.org/10.1074/jbc.M114.601328>
  34. Hua L, Cohen TS, Shi Y, Datta V, Hilliard JJ, Tkaczyk C, Suzich J, Stover CK, Sellman BR. MEDI4893\* Promotes survival and extends the antibiotic treatment window in a *Staphylococcus aureus* immunocompromised pneumonia model. *Antimicrob Agents Chemother* 2015; 59:4526-32; PMID:25987629; <http://dx.doi.org/10.1128/AAC.00510-15>
  35. Rouha H, Badarau A, Visram ZC, Battles MB, Prinz B, Magyarics Z, Nagy G, Mirkina I, Stulik L, Zerbs M, et al. Five birds, one stone: neutralization of  $\alpha$ -hemolysin and 4 bi-component leukocidins of *Staphylococcus aureus* with a single human monoclonal antibody. *Mabs* 2015; 7:243-54; PMID:25523282; <http://dx.doi.org/10.4161/19420862.2014.985132>
  36. Kato F, Sugai M. A simple method of markerless gene deletion in *Staphylococcus aureus*. *J Microbiol Methods* 2011; 87:76-81; PMID:21801759; <http://dx.doi.org/10.1016/j.mimet.2011.07.010>
  37. Romero-Steiner S, Libutti D, Pais LB, Dykes J, Anderson P, Whitin JC, Keyserling HL, Carlone GM. Standardization of an opsonophagocytic assay for the measurement of functional antibody activity against *Streptococcus pneumoniae* using differentiated HL-60 cells. *Clin Diagn Lab Immunol* 1997; 4:415-22; PMID:9220157
  38. Van Deventer JA, Wittrup KD. Yeast surface display for antibody isolation: library construction, library screening, and affinity maturation. *Methods Mol Biol Clifton NJ* 2014; 1131:151-81; PMID:24515465; [http://dx.doi.org/10.1007/978-1-62703-992-5\\_10](http://dx.doi.org/10.1007/978-1-62703-992-5_10)
  39. Ursby T, Unge J, Appio R, Logan DT, Fredslund F, Svensson C, Larsson K, Labrador A, Thunnissen MM. The macromolecular crystallography beamline I911-3 at the MAX IV laboratory. *J Synchrotron Radiat* 2013; 20:648-53; PMID:23765310; <http://dx.doi.org/10.1107/S0909049513011734>
  40. Kabsch W. XDS. *Acta Crystallogr D Biol Crystallogr* 2010; 66:125-32; PMID:20124692; <http://dx.doi.org/10.1107/S0907444909047337>
  41. Evans PR, Murshudov GN. How good are my data and what is the resolution? *Acta Crystallogr D Biol Crystallogr* 2013; 69:1204-14; PMID:23793146; <http://dx.doi.org/10.1107/S0907444913000061>
  42. Winn MD, Ballard CC, Cowtan KD, Dodson EJ, Emsley P, Evans PR, Keegan RM, Krissinel EB, Leslie AG, McCoy A, et al. Overview of the CCP4 suite and current developments. *Acta Crystallogr D Biol Crystallogr* 2011; 67:235-42; PMID:21460441; <http://dx.doi.org/10.1107/S0907444910045749>
  43. McCoy AJ, Grosse-Kunstleve RW, Adams PD, Winn MD, Storoni LC, Read RJ. Phaser crystallographic software. *J Appl Crystallogr* 2007; 40:658-74; PMID:19461840; <http://dx.doi.org/10.1107/S0021889807021206>
  44. Murshudov GN, Skubák P, Lebedev AA, Pannu NS, Steiner RA, Nicholls RA, Winn MD, Long F, Vagin AA. REFMAC5 for the refinement of macromolecular crystal structures. *Acta Crystallogr D Biol Crystallogr* 2011; 67:355-67; PMID:21460454; <http://dx.doi.org/10.1107/S0907444911001314>
  45. Emsley P, Lohkamp B, Scott WG, Cowtan K. Features and development of Coot. *Acta Crystallogr D Biol Crystallogr* 2010; 66:486-501; PMID:20383002; <http://dx.doi.org/10.1107/S0907444910007493>
  46. Winn MD, Murshudov GN, Papiz MZ. Macromolecular TLS refinement in REFMAC at moderate resolutions. *Methods Enzymol* 2003; 374:300-21; PMID:14696379; [http://dx.doi.org/10.1016/S0076-6879\(03\)74014-2](http://dx.doi.org/10.1016/S0076-6879(03)74014-2)
  47. Chen VB, Arendall WB, Headd JJ, Keedy DA, Immormino RM, Kapral GJ, Murray LW, Richardson JS, Richardson DC. MolProbity: all-atom structure validation for macromolecular crystallography. *Acta Crystallogr D Biol Crystallogr* 2010; 66:12-21; PMID:20057044; <http://dx.doi.org/10.1107/S0907444909042073>
  48. Krissinel E, Henrick K. Inference of macromolecular assemblies from crystalline state. *J Mol Biol* 2007; 372:774-97; PMID:17681537; <http://dx.doi.org/10.1016/j.jmb.2007.05.022>